

# Evidence of major dry mergers at $M_* > 2 \times 10^{11} M_\odot$ from curvature in early-type galaxy scaling relations?

Mariangela Bernardi<sup>1\*</sup>, Nathan Roche<sup>2</sup>, Francesco Shankar<sup>3</sup> & Ravi K. Sheth<sup>1,4</sup>

<sup>1</sup> *Department of Physics & Astronomy, University of Pennsylvania, 209 S. 33rd St., Philadelphia, PA 19104, USA*

<sup>2</sup> *Dipartimento di Astronomia, Università degli Studi di Bologna, via Ranzani 1, I-40127 Bologna, Italy*

<sup>3</sup> *Max-Planck-Institut für Astrophysik, Karl-Schwarzschild-Str. 1, D-85748, Garching, Germany*

<sup>4</sup> *Center for Particle Cosmology, University of Pennsylvania, 209 S. 33rd St., Philadelphia, PA 19104, USA*

19 September 2018

## ABSTRACT

For early-type galaxies, the correlations between stellar mass and size, velocity dispersion, surface brightness, color, axis ratio and color-gradient all indicate that two mass scales,  $M_* = 3 \times 10^{10} M_\odot$  and  $M_* = 2 \times 10^{11} M_\odot$ , are special. The smaller scale could mark the transition between wet and dry mergers, or it could be related to the interplay between SN and AGN feedback, although quantitative measures of this transition may be affected by morphological contamination. At the more massive scale, mean axis ratios and color gradients are maximal, and above it, the colors are redder, the sizes larger and the velocity dispersions smaller than expected based on the scaling at lower  $M_*$ . In contrast, the color- $\sigma$  relation, and indeed, most scaling relations with  $\sigma$ , are not curved: they are well-described by a single power law, or in some cases, are almost completely flat. When major dry mergers change masses, sizes, axis ratios and color gradients, they are expected to change the colors or velocity dispersions much less. Therefore, the fact that scaling relations at  $\sigma > 150 \text{ km s}^{-1}$  show no features, whereas the size- $M_*$ ,  $b/a$ - $M_*$ , color- $M_*$  and color gradient- $M_*$  relations do, suggests that  $M_* = 2 \times 10^{11} M_\odot$  is the scale above which major dry mergers dominate the assembly histories of early-type galaxies.

**Key words:** galaxies: formation

## 1 INTRODUCTION

Recent work (Bernardi et al. 2010b) has shown that the color-magnitude relation of early-type galaxies in the SDSS differs significantly from a pure power-law, curving downwards at low and upwards at large luminosities ( $M_r > -20.5$  and  $M_r < -22.5$ , respectively). This is also true of the color-size relation, and is even more apparent with stellar mass, where the corresponding mass scales are  $M_* < 3 \times 10^{10} M_\odot$  and  $M_* > 2 \times 10^{11} M_\odot$ , respectively. The upwards curvature at the massive end does not appear to be due to stellar population effects. Curvature in the color-luminosity (or color- $M_*$ ) relation at the faint end was noticed before (e.g. Graham 2008; Skelton et al. 2009); the curvature at bright end is the new finding of Bernardi et al. (2010b).

Curvature at the low mass end using other parameters (e.g. surface brightness) has been noticed before as well (e.g. Kauffmann et al. 2003; Shankar et al. 2006); the subject of this Letter is to analyse non-linear scaling relations at the high mass end, extending the analysis of Hyde & Bernardi

(2009). We show that the curvature in the color- $M_*$  relation coincides with curvature in other relations with  $M_*$ . However, when  $M_*$  is replaced with velocity dispersion, then there is little curvature. Although curvature in scaling relations does not imply a change in the physics which sets the relations (e.g. Graham & Guzman 2003; Graham 2010), we argue that our findings suggest that major dry mergers dominate the mass growth at  $M_* > 2 \times 10^{11} M_\odot$ .

Our results are based on two different ways of selecting early-type samples from the SDSS database. One follows Hyde & Bernardi (2009): the image must be round ( $b/a > 0.6$ ) and the light profile shape must be well-fit by a deVaucouleurs profile ( $\text{fracDev} = 1$ ). The other is a simple cut on how centrally concentrated the surface brightness is ( $C_r > 2.86$ ). The former method produces a sample that is more purely elliptical; the latter contains many edge-on disks. See Bernardi et al. (2010a) for a more detailed discussion of these selection criteria, and of the SDSS photometric and spectroscopic parameters which we use below. Where necessary, we have assumed a spatially flat background cosmology with energy density dominated by

\* E-mail: bernardm@physics.upenn.edu

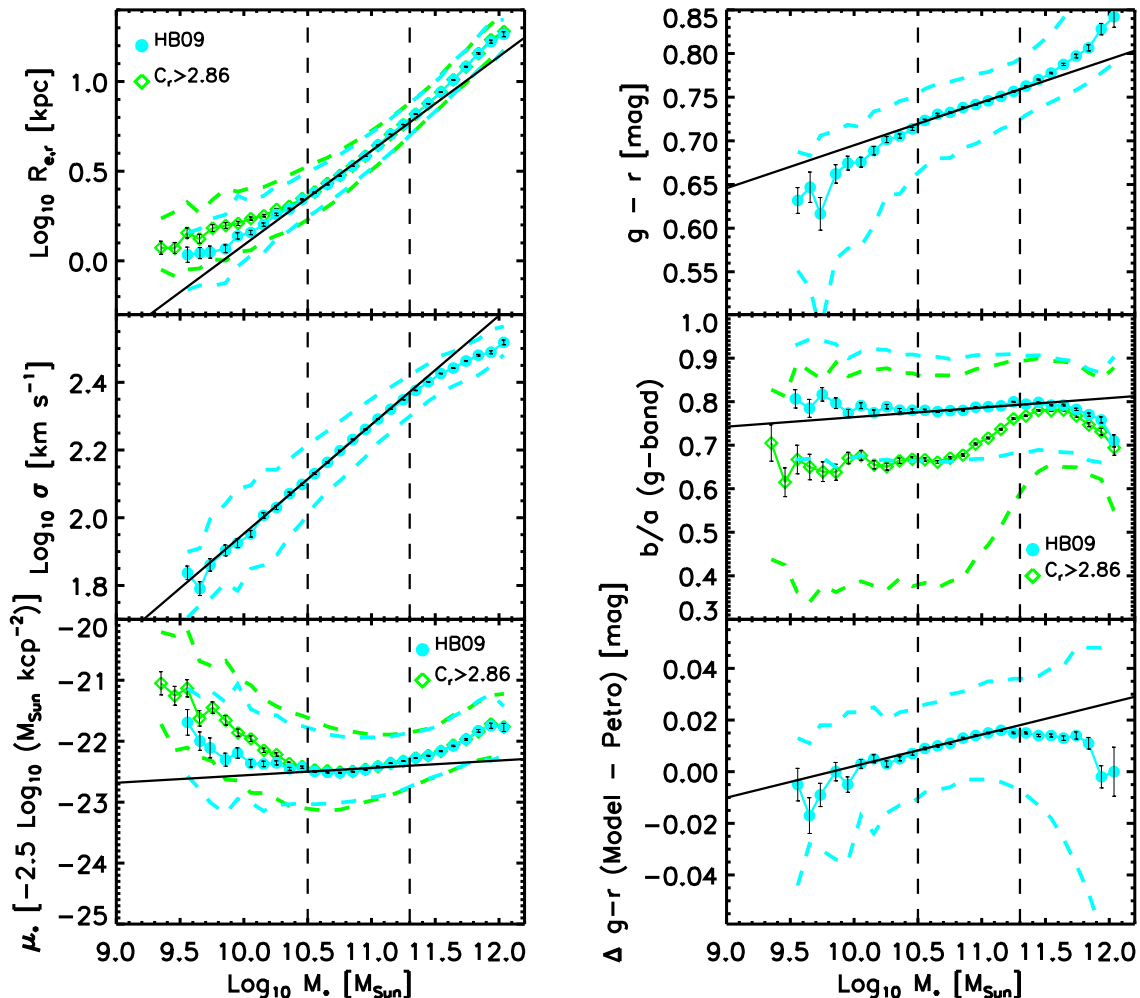


**Figure 1.** Curvature in the correlations between stellar mass and (from top to bottom, left) size, velocity dispersion and surface brightness, and color, axis ratio, and color gradient (top to bottom, right), in the Hyde-Bernardi sample. The vertical dashed lines mark the scales where some of the relations change slope:  $M_* = 3 \times 10^{10} M_\odot$  and  $2 \times 10^{11} M_\odot$ , which correspond approximately to  $M_r = -20.5$  and  $-22.5$ . Scalings in a sample selected to have  $C_r > 2.86$  are shown only where they differ from the scalings in the Hyde-Bernardi sample.

a cosmological constant  $\Lambda = 0.7$ , with a Hubble constant  $H_0 = 70 \text{ km s}^{-1} \text{ Mpc}^{-1}$  at the present time.

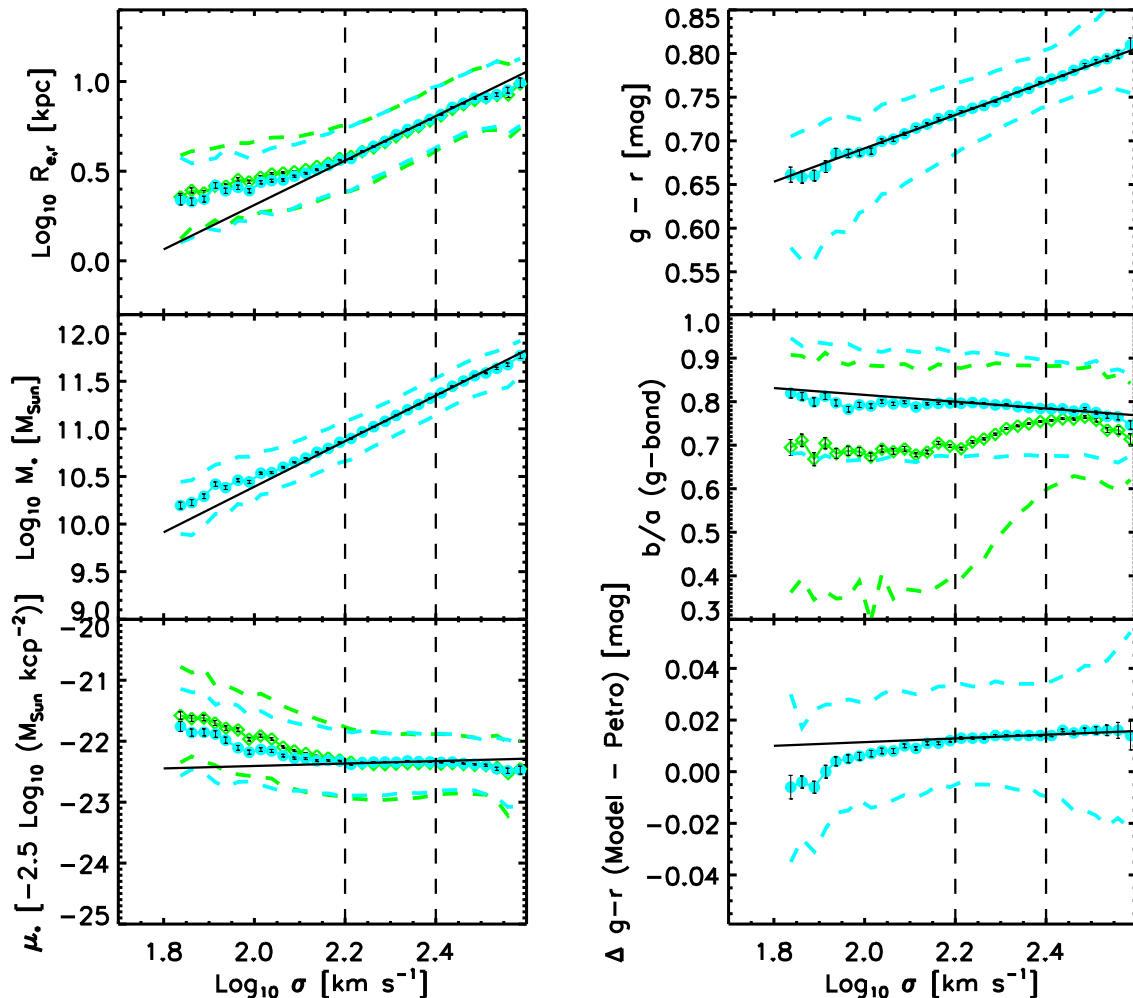
## 2 CURVATURE IN RELATIONS WITH $M_*$ , BUT NOT WITH $\sigma$

Figure 1 shows correlations between stellar mass and (from top to bottom, left) size, velocity dispersion and surface brightness, and color, axis ratio, and color gradient (top to bottom, right), in the Hyde-Bernardi sample. (We discuss how we define the gradient in Section 3.2.) None of these correlations are pure power laws. Although the curvature at  $\log_{10} M_*/M_\odot < 10.5$  is interesting – galaxies at the faint, low mass end ( $M_r \geq -20.5$ ,  $\log_{10}(M_*/M_\odot) \leq 10.5$ ) tend to curve towards bluer colors, larger sizes, fainter surface brightnesses, smaller axis ratios and color gradients – in what follows, we will focus on what appears to be a transition mass scale at higher masses. At  $\log_{10} M_*/M_\odot > 11.3$ ,

the relations curve towards larger sizes, smaller than expected velocity dispersions, fainter surface brightnesses (left panels), and smaller axis ratios and smaller color-gradients (right panels). This is precisely the mass scale on which the color- $M_*$  relation curves towards redder colors (top right panel).

Figure 2 shows that when  $M_*$  is replaced with velocity dispersion, then there is little curvature at  $\log \sigma/\text{kms}^{-1} > 2.2$ . In fact, the correlations with surface brightness, color gradient and axis ratio are almost completely flat. (That surface brightness and  $\sigma$  are uncorrelated was noted by Bernardi et al. 2003.) The fact that there is no feature at the largest  $\sigma$  in any of these relations, despite clear features in the scalings with  $M_*$ , is what has motivated this Letter.

In this context, it is important to note that the relation between  $M_{\text{dyn}} \propto R\sigma^2$  and luminosity or  $M_*$  is very well described by a single power-law over the entire range: the curvature in the sizes and velocity dispersions cancel (Fig-



**Figure 2.** Curvature in the correlations between velocity dispersion and (from top to bottom, left) size, stellar mass and surface brightness, and color, axis ratio, and color gradient (top to bottom, right), in the Hyde-Bernardi sample. The dashed lines mark the scales where one would expect to see a change in the slope of the relations based on Figure 1. Scalings in a sample selected to have  $C_r > 2.86$  are shown only where they differ from the scalings in the Hyde-Bernardi sample.

ure 3). Presumably, this is because the objects we observe are virialized, whatever their merger histories.

### 3 DISCUSSION

Major dissipationless mergers are expected to change the sizes in proportion to the masses, but to leave the velocity dispersions and colors unchanged. In contrast, minor dissipationless mergers produce larger fractional changes in size than in mass, and decrease the velocity dispersions and colors (see Appendix C in Bernardi et al. 2010b for details). Therefore, the curvature in the correlations between  $M_*$  and other parameters as size,  $\sigma$  and color, which have been noticed before, have all been discussed in this context (e.g. Davies et al. 1983; Matkovic & Guzman 2005; Bernardi et al. 2007; Hyde & Bernardi 2009; Bernardi et al. 2010a,b). What is new here is the recognition that these all occur at the same mass scale, that this mass scale is also important

for axis-ratios and color-gradients, and, significantly, that the curvature is absent when  $M_*$  is replaced by  $\sigma$ .

#### 3.1 Axis-ratios

The  $b/a - M_*$  relation (right center panel of Figure 1) deserves further comment. Van der Wel et al. (2009) report that the width of the  $b/a$  distribution changes at  $\log(M_*/M_\odot) \sim 10.5$ . They interpret this as evidence that, above this mass, assembly histories are dominated by major mergers. Our results suggest this is not the full story.

In Figure 1 we have shown two versions of this relation, because the Hyde-Bernardi selection requires  $b/a > 0.6$ . In this sample,  $b/a$  decreases at  $\log(M_*/M_\odot) > 11.3$ . However, notice that this decrease is even more marked in the sample selected to have  $C_r > 2.86$ , where no cut on  $b/a$  is applied. Compared to the Hyde-Bernardi sample, this sample has considerably smaller  $b/a$  at small  $M_*$ . Bernardi et al. (2010a) show that this is primarily due to an increased incidence

of disks and contamination by SAs, because the  $C_r > 2.86$  sample is not as purely elliptical/early-type as the Hyde-Bernardi sample. We believe this change in morphological mix is the primary reason why Van der Wel et al. saw what they did.

We believe the real feature of interest is the drop in  $b/a$  at  $\log(M_*/M_\odot) > 11.3$  where (Bernardi et al. 2010a show that) morphological mix is no longer an issue. Van der Wel et al. also see this drop, but they dismiss it. Instead, we believe the narrowing of the distribution at  $\log(M_*/M_\odot) \sim 10.5$  marks the transition from dissipational to dissipationless histories, or a change in relative importance of SN and AGN feedback (e.g. Kauffmann et al. 2003; Shankar et al. 2006), while the decrease in  $b/a$  at  $\log(M_*/M_\odot) > 11.3$  marks the transition to major dry mergers. This decrease has been expected for some time (see González-García & van Albada 2005; Boylan-Kolchin et al. 2006; Ragone-Figueroa & Plienis 2007; Ragone-Figueroa et al. 2010) – it was first found by Bernardi et al. (2008). This is thought to indicate an increasing incidence of major radial mergers, since these would tend to result in more prolate objects.

### 3.2 Color gradients

The right bottom panel of Figure 1 shows that color-gradients — here defined to be the difference between the *model* and *Petrosian* colors — are maximal at  $\log(M_*/M_\odot) \sim 11.3$ . (The former are approximately the color within the half-light radius, whereas the latter are more closely related to the ratio of the total luminosities in  $g$  and  $r$ , so correspond to larger scales.) This is consistent with Figure B1 of Bernardi et al. (2010b), who used the same definition of color gradient. It is also consistent with Roche et al. (2010), who used a different estimator of the gradient: the ratio of the half-light sizes in the  $g$  and  $r$  bands. As we discuss below, we believe that the appearance of this same mass scale is again signaling the onset of major dry mergers.

Whereas major mergers are expected to decrease color gradients (e.g. Di Matteo et al. 2009), minor mergers should not change the gradients significantly (Kobayashi 2004) or they may enhance them slightly. This is because the smaller bluer object involved in the minor merger is expected to deposit most of its stars at larger distances from the center of the object onto which it merged. (If it had its own gradient, then the bluest of its stars would have been deposited at the largest radii.)

As a simple check of this argument, note that major mergers, which double  $M_*$ , do not change  $\sigma$  (Appendix C of Bernardi et al. 2010b). Therefore, a plot of color gradient versus  $\sigma$  should show less of a feature than when gradients are plotted versus  $M_*$ . This is indeed what we see in Figure 2 (right bottom panel) – the correlation is almost flat at  $\sigma > 150 \text{ km s}^{-1}$ . Such a plot should also show greater scatter, since a range of merger histories, hence gradients, can all have the same  $\sigma$ . While we do see this increase in scatter, note that the scatter in the gradient- $M_*$  relation grows even more dramatically – something that is not easily explained. On the other hand, the major merger picture also provides a natural explanation for why none of the scaling relations in Figure 2 show any feature at  $\log \sigma / \text{km s}^{-1} > 2.2$ , and those that are most clearly sensitive to merger histories are almost completely flat.

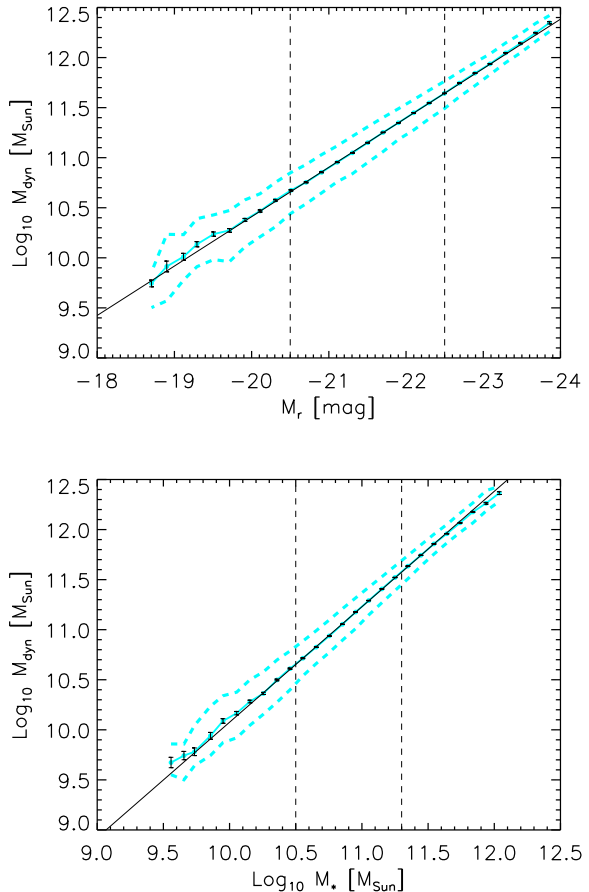


**Figure 3.** No curvature in the correlations between dynamical mass and luminosity (top) and stellar mass (bottom).

Mergers are not the only way to produce or alter color gradients. In some models, gradients are related to feedback and winds (Pipino et al. 2010). Our demonstration that gradients scale differently with  $M_*$  than with  $\sigma$  may have interesting implications for such models. In addition, producing the downturn we see at  $\log(M_*/M_\odot) > 11.3$  is an interesting challenge for such models, as is relating this to the changes in size,  $\sigma$  and  $b/a$  we have found. Because the major dry merger model provides a simple framework for understanding all these relations, our results suggest that  $M_* > 2 \times 10^{11} M_\odot$  is the scale above which major dry mergers dominate the assembly history.

## 4 IMPLICATIONS

We have found that a variety of early-type galaxy scaling relations – the size- $M_*$ ,  $b/a$ - $M_*$ , color- $M_*$  and color gradient- $M_*$  relations – all show departures from a pure power-law at  $M_* = 2 \times 10^{11} M_\odot$ , whereas there is no such feature when  $M_*$  is replaced with  $\sigma$ . Since major dry mergers are expected to change the sizes, axis ratios and color gradients of galaxies while leaving the velocity dispersion and color unchanged, our findings suggest that the total stellar mass in early-types with  $M_* > 2 \times 10^{11} M_\odot$  today must have grown primarily by relatively recent major dry mergers. In Bernardi et al.

(2010b), we argue that such mergers may be required to reconcile the  $z \sim 1$  counts of objects with  $M_* > 2 \times 10^{11} M_\odot$  with those at  $z \sim 0$ .

This particular mass scale also appears in analyses of a local sample (higher quality data, but significantly smaller sample), where it is identified with the transition to dry mergers (see page 270 and related discussion in Kormendy et al. 2009). It is special in hierarchical models also. Figure 3 of Guo & White (2008) shows that below  $1.6 \times 10^{11} M_\odot$  star-formation has been a significant part of the mean stellar mass growth rate (much of it through wet mergers), whereas the stellar mass growth at masses above this occurs only through dry mergers. See Hopkins et al. (2008) and Eliche-Moral et al. (2010a,b) for other arguments suggesting dry mergers since  $z \sim 1$  are a natural and necessary part of the assembly history at  $M_* > 2 \times 10^{11} M_\odot$ . While it is reassuring that many lines of study all identify this same mass scale, we feel it worth emphasizing that our analysis suggests that above this mass scale, the mergers were not just dry – they were major. In this respect, there is some tension between our conclusions, and recent work which argues that although the mass in the central kpc or so of early-type galaxies has not grown since  $z \sim 2$ , the half-light radii have increased by more than a factor of two. This suggests that, since  $z < 2$ , mass has been added to the outer regions only: this sort of inside-out scenario for the growth is most easily understood if the mergers were minor (e.g. Lapi & Cavaliere 2009; Cook et al. 2009; Bezanson et al. 2009). However, as Tiret et al. (2010) note, the observation of constant mass in the central regions does not, by itself, exclude major mergers. In the simulations of Gao et al. (2004), as an object assembles its mass through major dry mergers, the mix of particles in the central regions can change dramatically, even though the total mass in the central regions remains constant. Our finding that color-gradients are erased at large masses may be indicating that this is indeed what happens at  $M_* > 2 \times 10^{11} M_\odot$ .

Finally, it is interesting to ask how BCGs, which are amongst the most massive objects in the local universe, fit into this picture? Compared to non-BCGs of similar mass or luminosity, their colors are slightly redder (Roche et al. 2010; Figure 10 in Bernardi et al. 2010b), they have smaller color gradients (Roche et al. 2010), and slightly larger sizes (Bernardi 2009). Whereas the first two are in agreement with our major merger picture, the last suggests more size growth than is usually associated with major mergers. Hence, it may be better to think of BCG formation as a two step process. In the first, the major mergers which result in the object becoming a BCG erase its color gradient (and decrease  $b/a$  – Bernardi et al. 2008); thereafter, minor mergers puffed up its size. Tidal stripping during the minor merger may also have contributed to the formation of intracluster light in its host halo (Bernardi 2009; Bernardi et al. 2010b). This two step picture is in striking agreement with a detailed analysis of the age, metallicity and abundance gradients of BCG NGC 4889 (Coccatto et al. 2010).

## ACKNOWLEDGMENTS

We are grateful to Simona Mei for help, encouragement, and for urging us to reorganize how we present our findings.

MB thanks Meudon Observatory, and RKS thanks the IPhT at CEA-Saclay, for their hospitality during the course of this work. MB is grateful for support provided by NASA grant ADP/NNX09AD02G; FS acknowledges support from the Alexander von Humboldt Foundation; RKS is supported in part by nsf-ast 0908241.

## REFERENCES

- Bernardi M., et al. 2003, *AJ*, 125, 1849  
 Bernardi M., Hyde J. B., Sheth R. K., Miller C. J., Nichol R. C. 2007, *AJ*, 133, 1741  
 Bernardi, M., Hyde, J. B., Fritz, A., Sheth, R. K., Gebhardt, K. & Nichol, R. C. 2008, *MNRAS*, 391, 1191  
 Bernardi M., 2009, *MNRAS*, 395, 1491  
 Bernardi M., Shankar, F., Hyde, J. B., Mei, S., Marulli, F. & Sheth, R. K. 2010a, *MNRAS*, 404, 2087  
 Bernardi M., Roche N., Shankar F., Sheth R. K., 2010b, *MNRAS*, submitted (arXiv:1005.3770)  
 Bezanson R., van Dokkum P. G., Tal T., Marchesini D., Kriek M., Franx M., Coppi P., 2009, *ApJ*, 697, 1290  
 Boylan-Kolchin M., Ma C.-P., Quataert E., 2006, *MNRAS*, 369, 1081  
 Coccatto, L., Gerhard, O. & Arnaboldi, M. 2010, *MNRAS*, 407, L26  
 Cook M., Lapi A. & Granato G. L., 2009, *MNRAS*, 397, 534  
 Davies, R. L., Efstathiou, G., Fall, S. M., Illingworth, G. & Schechter, P. L. 1983, *ApJ*, 266, 41  
 Di Matteo P., Pipino A., Lehnert M. D., Combes F., Semelin B., 2009, *A&A*, 499, 427  
 Eliche-Moral, M. C., Prieto, M., Gallego, J., Barro, G., Zamorano, J., López-Sanjuan, C., Balcells, M., Guzmán, R. & Muñoz-Mateos, J. C. 2010, *A&A*, 519, 55  
 Eliche-Moral, M. C., Prieto, M., Gallego, J. & Zamorano, J. 2010, *ApJ*, submitted (arXiv:1003.0686)  
 Gao, L., Loeb, A., Peebles, P. J. E., White, S. D. M. & Jenkins, A. 2004, *ApJ*, 614, 17  
 González-García A. C., van Albada T. S., 2005, 361, 1043  
 Graham, A. W. & Guzmán, R. 2003, *AJ*, 125, 2936  
 Graham A. W., 2008, *ApJ*, 680, 143  
 Graham A. W., 2010, (arXiv:1009.5002)  
 Guo, Q. & White, S. D. M. 2008, *MNRAS*, 384, 2  
 Hopkins, P. F., Cox, T. J., Keres, Dusan & Hernquist, L. 2008, *ApJS*, 175, 390  
 Hyde J. B., Bernardi M., 2009, *MNRAS*, 394, 1978  
 Kauffmann, G., et al. 2003, *MNRAS*, 341, 33  
 Kobayashi C., 2004, *MNRAS*, 347, 740  
 Kormendy, J., Fisher, D. B., Cornell, M. E. & Bender, R. 2008, *ApJS*, 182, 216  
 Lapi A. & Cavaliere A., 2009, *ApJ*, 692, 174  
 Matković, A. & Guzmán, 2005, *MNRAS*, 362, 289  
 Pipino A., D’Ercole A., Chiappini C., Matteucci F., 2010, *MNRAS*, in press (arXiv:1005.2154)  
 Ragono-Figueroa, C. & Plionis, M. 2007, *MNRAS*, 377, 1785  
 Ragono-Figueroa, C., Plionis, M., Merchán, M., Gottlöber, S. & Yepes, G. 2010, *MNRAS*, 407, 581  
 Roche, N., Bernardi, M. & Hyde, J. B. 2010, *MNRAS*, 407, 1231  
 Shankar F., Lapi A., Salucci P., De Zotti G., Danese L. 2006, *ApJ*, 643, 14  
 Skelton, R. E., Bell, E. F. & Somerville, R. S. 2009, *ApJL*, 699, 9  
 Tiret, O., Salucci, P., Bernardi, M., Maraston, C. & Pforr, J. 2010, *MNRAS*, in press (arXiv:1009.5185)  
 Van der Wel A., Rix H.-W., Holden, B. P., Bell E. F. & Robaina, A. R. 2009, *ApJL*, 706, 120